ISSN 0252-1075
Contribution from IITM
Research Report No. RR-108

Indian Ocean Dipole Simulation Using Modular Ocean Model

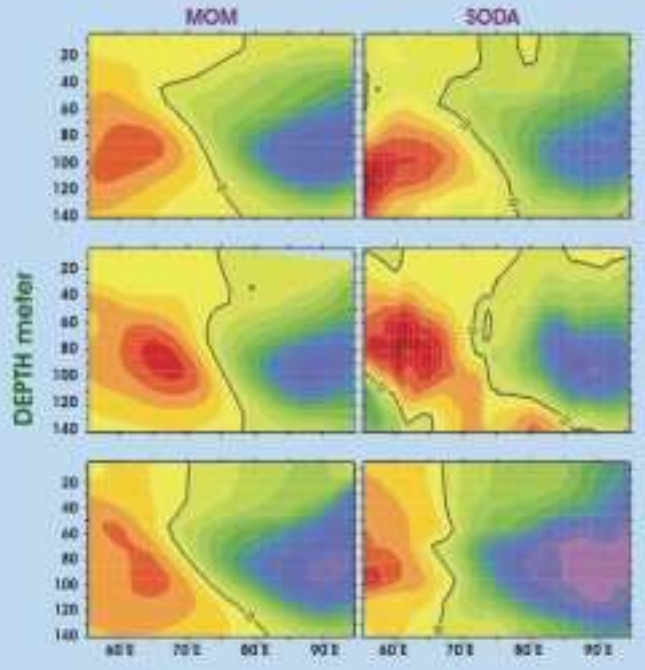

July 2005

Indian Institute of Tropical Meteorology
Pune - 411 008, India

ISSN 0252-1075
Contribution from IITM
Research Report No. RR-108

Indian Ocean Dipole Simulation Using Modular Ocean Model

B. Thompson, C. Gnanaseelan

and

P.S. Salvekar

July 2005

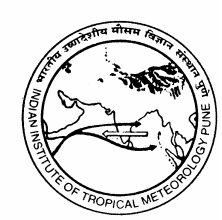

Indian Institute of Tropical Meteorology
Dr. Homi Bhabha Road, Pashan Pune - 411 008
Maharashtra, India

E-mail : lip@tropmet.res.in Fax : 91-020-25893825
Web : http://www.tropmet.res.in Telephone : 91-020-25893600

Contents

Abstract

1. Introduction 1

2. Model and Methodology 3

2.1 Datasets Used 5

3. Results and Discussions 5

3.1 Simulation of SST 6

3.2 SST Variability During IOD events 6

3.3 Subsurface Temperature Variability 8

3.4 Simulation of North and Equatorial Indian Ocean Circulation 8

4. Summary 11

Appendix A 12

Acknowledgements 13

References 14

Figures 16

Indian Ocean Dipole Simulation Using Modular Ocean Model

B. Thompson, C. Gnanaseelan and P.S. Salvekar

ABSTRACT

The GFDL Modular Ocean Model version 4 (MOM4) forced with interannually varying surface forcing has been used to simulate the dipole mode events in the tropical Indian Ocean. The model is able to simulate the dipole mode events occurred during the simulation period 1958-2000. The model simulations are validated and compared with various data sets such as HadISST, SODA and ECCO. The surface and subsurface warming/cooling associated with dipole mode events are reproduced by the model. The maximum temperature anomalies are observed at depth of 80-100m in the equatorial Indian Ocean in western and eastern basins. The observed western equatorial Indian Ocean warming/cooling was weaker than the corresponding cooling/warming in the south eastern Indian Ocean both in the surface and subsurface. The surface and subsurface current variability during dipole mode events have been well captured by the model. The presence of strong upwelling in the eastern equatorial Indian Ocean and downwelling in western tropical Indian Ocean were evident in the model analysis of vertical velocities.

1. Introduction

The surface of ocean forms a boundary between atmosphere and ocean, where exchange of heat and momentum fluxes takes place between these two systems. The variability of sea surface parameters like Sea Surface Temperature (SST), sea surface height and surface currents is primarily driven by the surface wind, the short wave radiation and the turbulent heat fluxes. Besides these constraints the three dimensional advection and internal dynamical processes occurring in the ocean basin is also critical in determining the sea surface parameters (Waliser et al., 2003). The oceans largely remain to be data sparse region. Even though the atmospheric data over ocean is also sparse (as compared to land), it has improved in the recent years with the satellite observations. However the remote sensing techniques have limitations in observing the ocean below a few centimeters, and also they are limited to only few oceanic parameters such as SST and sea surface height anomaly. The relative abundance of atmospheric data can be imposed in a state-of-the-art Ocean General Circulation Model (OGCM) frame work and more realistic simulation of oceanic geophysical parameters can be done in surface and interior of oceans. In this scenario the three dimensional OGCMs provide a most reliable estimate of parameters in the surface and interior of oceans. The lack of currents and salinity observations in the surface and interior and temperature observations in the interior of oceans has highlighted the necessity of well parameterised ocean models. The inventory of high performance computing systems gave the model developers the freedom to reduce unrealistic approximations and assumptions from models. This in fact helped to reduce the inaccuracies in the model simulations to a great extent. Here we have used an OGCM to study the surface and subsurface variability in the equatorial Indian Ocean during Indian Ocean Dipole mode events.

The north Indian Ocean is dominantly forced by the monsoonal winds. The seasonal reversal of winds over the northern and equatorial Indian Ocean attributes to the reversal of surface and near surface oceanic circulations. Because of this intense monsoonal shift the representation of the Indian Ocean as a steady state system is highly problematic. The increased precipitation over tropical eastern Africa and western

Indian ocean, while severe drought situation over Indonesian Islands during 1961 and 1997-1998 (Saji et al., 1999; Webster et al., 1999) widely gained attention of atmosphere and ocean researchers. Normally Equatorial Indian Ocean (EIO) will be warmer in the eastern part compared to west. However during these abnormal years anomalous pattern of SST gradient was observed. Saji et al., (1999), through analysis of long term SST data sets, observed the existence of a dipole/zonal mode structure in the SST anomalies in the equatorial Indian Ocean. This dipole/zonal mode structure is primarily characterised by abnormal positive SST anomaly in the western equatorial Indian Ocean and negative SST anomalies in the east equatorial Indian Ocean. Associated with the reversal of SST gradient, the weak climatological equatorial westerly winds are replaced by easterly winds (Webster et al., 1999). Masson et al., (2002) observed that during the fall of 1997, equatorial Indian Ocean is marked by westward wind stress of 0.2 N/m^2 - 0.3 N/m^2 resulting anomalous cooling in the east and warming in the west equatorial Indian Ocean. In contrast 1996 is characterised by positive SST anomalies in the east equatorial Indian Ocean and negative SST anomalies in the western part. This unusual warming/cooling in the western EIO and unusual cooling/warming in the eastern EIO is denoted as Indian Ocean Dipole/zonal Mode (IOD) events (Saji et al., 1999; Webster et al., 1999). Positive IOD years are characterised by anomalous warming (cooling) in western (eastern) EIO. A reversal of these anomalies happens during negative phase of IOD. This basin scale SST anomalies represent one of the dominant modes of SST variability in the Indian Ocean. The variability of SST in the Indian Ocean has been extensively discussed through several studies (Nicholls, 1989; Behera et al., 1999 and 2000; Murtugudde et al., 2000; Iizuka et al., 2000; Vinayachandran et al., 2002). The impact of IOD on the climate of region around Indian Ocean has been widely described (Zubair et al., 2003; Behera and Yamagata, 2003; Saji and Yamagata, 2003). Rao et al., (2002) discussed about the subsurface temperature variability in the Indian Ocean during dipole events using observational data and OGCM simulations.

The presence of a thick barrier layer in the east equatorial Indian Ocean has been reported by several authors (Godfrey et al., 1999; Masson et al., 2002). The generation and further survival of this barrier layer largely depends on the intrusion of eastward

flowing equatorial jets (Wyrtki Jets) into the east equatorial Indian Ocean (Masson et al., 2002). During positive IOD years EIO is distinguished by the weakening or reversal of Wyrtki Jets (Murtugudde et al., 2000, Vinayachandran et al., 2002). The variability in barrier layer forced by these abnormal equatorial currents influences the formation and growth of IOD events. The unusual absence of barrier layer off Sumatra during fall of positive IOD events aids the cooling of SST via Sumatra upwelling (Murtugudde et al., 2000; Annamalai et al., 2003; Masson et al., 2004). While the presence of thick barrier layer induces positive SST anomalies in the western Indian Ocean by inhibiting the entrainment cooling.

2. Model and Methodology

The Ocean General Circulation Model used for this study is the Geophysical Fluid Dynamics Laboratory (GFDL) Modular Ocean Model Version 4 (MOM4p0c) (Griffies et al. 2003). MOM is a 3 dimensional, z – coordinate, free surface OGCM, which evolved from numerical ocean models developed in the 1960's - 1980's by Kirk Bryan and Mike Cox at GFDL. MOM is designed primarily as a tool for studying the ocean climate system. MOM is a finite difference version of the ocean primitive equations, which govern much of the large scale ocean circulation. As described by Bryan (1969) the equations consist of Navier - Stokes equations subject to hydrostatic and Boussinesq approximations. The fundamental model Equations are

$$u_t = -\nabla.\left(u\overline{U}\right) + v\left(f + \frac{u\tan\phi}{a}\right) - \left(\frac{1}{a\rho\cos\phi}\right)P_\lambda + \left(k_m u_z\right)_z + F^u \qquad \text{---- (1)}$$

$$v_t = -\nabla.\left(v\overline{U}\right) + u\left(f + \frac{u\tan\phi}{a}\right) - \left(\frac{1}{a\rho}\right)P_\phi + \left(k_m u_z\right)_z + F^v \qquad \text{---- (2)}$$

$$w_t = -\nabla_h.U_h \qquad \text{---- (3)}$$

$$P_z = -\rho g \qquad \text{---- (4)}$$

$$\theta_t = -\nabla.\left(U\theta + F(\theta)\right) \qquad \text{---- (5)}$$

$$S_t = -\nabla.\left(U_s + F(s)\right) \qquad \text{---- (6)}$$

$$\rho = \rho(\theta, S, P) \qquad \text{---- (7)}$$

Where ϕ is latitude, λ is longitude, g = 9.806 m/s^2, a = radius of earth = 6371 x 10^3 m, f = Coriolis parameter = 2 Ω sinϕ, Ω = earths angular velocity = 7.292 x 10^{-5}. The formulation of heat fluxes are given as appendix A.

The model bottom topography is represented using the partial cells of Pacanowski and Gnanadesikan (1998). In situ density is a function of the local potential temperature, salinity, and hydrostatic pressure. Horizontal friction scheme is based on the shear-dependent Smagorinsky viscosity. The vertical mixing in the model is handled through K Profile Parameterisation Scheme (Large et al. 1994) having local and non - local mixing with Bryan-Lewis Background Diffusivity (Bryan 1979).

The model region is 30^{o}E to 120^{o}E and 40^{o}S to 25^{o}N having 30 vertical levels with upper 150 m has 10 m resolution and the vertical thickness gradually increases to a maximum of 712m at 5200m depth. Model has a constant zonal resolution of 1^o and meridional resolution varying from 0.3353 at equator to 0.7^o at 25^{o}N and 1.5^o at 40^{o}S. The model has been provided with realistic topography of 0.5^o resolution. Sponge layers of thickness 4^o applied in the eastern and southern boundaries where model temperatures and salinities are relaxed towards Levitus (1998) data. The model was initialised with annual climatologies of temperature and salinity from Levitus (1998) and forced with climatological downwelling shortwave and longwave radiation, 10m wind fields, specific humidity, air temperature and surface precipitation from NCAR Climatology. Chlorophyll-a climatology computed from SeaWiFS satellite for the period 1999-2001 is provided to handle short wave penetration. After 20 years of spin up model has been integrated for a period of 43 years from 1958 – 2000 with NCAR corrected interannual datasets (Large and Yeager 2004) of daily downwelling shortwave and longwave radiation, 6- hourly 10m wind fields, specific humidity, air temperature and monthly precipitation. During the interannual simulation the surface fluxes are corrected on 30 day timescale using seasonal climatological temperature and salinity.

2.1 Datasets Used

The Simple Ocean Data Assimilation (SODA) datasets are used for comparison with model simulations. The SODA version used here is SODA_1.2, which is a UMD reanalysis product using an eddy-permitting global model based initially on POP_1.3 numerics and SODA procedure. The horizontal resolution of POP on the equator is 28km x 44km reducing to an approximately uniform 25km x 25 km in the western North Atlantic. Vertically, it contains 40 levels, from ocean surface to about 5500m. The optimum interpolation analysis was done with SODA procedure every 10 days on 1 by 1 degree resolution. The observed data of SST, subsurface temperature and salinity were used in the analysis. More details about this data set please refer to http://www.atmos.umd.edu/~ocean/soda1.2.pdf.

Estimating Climate and Circulation of the Ocean (ECCO) products also provides high quality assimilated data sets. The data assimilated include sea surface height from Earth Resource Satellite (ERS) and TOPEX/Poseidon, monthly Reynolds and Tropical Rainfall Measuring Mission Microwave Imager SST, NCEP surface forcing, monthly Levitus climatology, World Ocean Circulation Experiment hydro graphic sections, Sea Surface Salinity observations, Expendable Bathy Thermograph and Tropical Ocean Global Atmosphere Tropical Atmosphere Ocean temperature profiles, temperature and salinity from P-ALACE and ARGO floats, monthly wind stress from ERS/NSCAT/QSCAT and mean 15m drifter velocities. More details about ECCO data described in ECCO report No. 20 (http://www.ecco-group.org/report/report_20.pdf).

For the validation and comparison of model simulated SST, HadISST v.1.1 is used. In situ sea surface observations and satellite derived estimates at the sea surface are included in the HadISST Global Ocean Surface Temperature analysis (Rayner et al. 2003).

3. Results and Discussions

3.1 Simulation of SST

The ocean model simulations give immense opportunity in understanding the thermodynamics and dynamics of oceans where the observations are sparse. However the model simulations need to be thoroughly validated with available observations. Figure 1 shows the comparison of model simulated seasonal climatologies of SST with Levitus (1998) climatology for winter (a), spring (b), summer (c) and fall seasons (d). The model climatology is calculated for the entire simulation period from 1958 - 2000. The model accuracy has been tested using root mean square (RMS) error (between model and observation). The model SST shows an RMS difference of 0.39, 0.27, 0.39 and 0.32^{o}C for the respective seasons with Levitus climatology and 0.25 ^{o}C for the annual climatology. The climatological features like winter cooling of the northern Arabian Sea, the pre-monsoon warming of northern Indian Ocean and cooling of western Arabian Sea during monsoon season are well simulated by the model. The anomaly correlation between seasonal SST of model and SODA for the period 1958-2000 is shown in figure 2 (Left panel). The correlation below 99% confidence level has been shaded. The model SST anomalies show good agreement with SODA. The correlation is observed to be less near the Somali coast and central Bay of Bengal during summer season. The strong monsoonal effects may be responsible for that. The RMS difference between model SST anomalies and SODA SST anomalies for winter, spring, summer and fall seasons are represented in figure 2 (right panel). The difference is more in the Somali coast during summer and fall seasons. RMS difference of 0.5 ^{o}C is seen south of 10 ^{o}S during summer season. The intensity of SST cooling/warming in the model during the dipole mode years is observed to be slightly different from SODA. This may be the reason for the larger RMS error (about 0.5 ^{o}C) in the eastern tropical Indian Ocean in fall season. However the RMS error is very small (<0.35 ^{o}C) in the entire northern Indian Ocean during winter and spring seasons.

3.2 SST Variability During IOD events

The intensity of IOD events can be represented with a simple time series index suggested by Saji et al., (1999). The dipole mode index is the difference between SST anomalies averaged in the western basin (50^oE to 70^oE, 10^oS to 10^oN) and eastern basin (90^oE to 110^oE, 10^oS to equator). The dipole mode index calculated from model SST, HadISST and SODA data are showed in the figure 3. The time series analysis of the normalised anomalies indicates that the strong positive IOD years 1961, 1963, 1967, 1972, 1977, 1982, 1994 and 1997 are all well simulated by the model. Model DMI is well comparable with HadISST. Considerable difference in DMI is seen in 1961 and 1963. In 1961 both model and SODA over estimates the dipole mode index (DMI). The EOFs of SST anomalies show that the SST variability of the Indian Ocean is dominantly described by two modes (Figure 4). The EOF1 explains 37% of total variability, which is of uniform polarity (negative) in the entire tropical Indian Ocean. This mode corresponds to ENSO variability. The second mode gives 14% of total variability. The second mode corresponds to dipole mode, which shows positive loading in south eastern tropical Indian Ocean and negative loading in western tropical Indian Ocean. The EOF analysis of HadISST and SODA data sets for the same period (1958-2000) shows 38% and 26% of total variability for the first mode and 9% and 7% of total variability for the second mode respectively (figures not shown).

The time of origin of IOD varies in different years. The initial signals of anomalous cooling/warming of east and central EIO and warming/cooling of eastern EIO appears in May - August. During 1961 the eastern cooling started in May. However during 1994 the cooling began in June and May in 1997. The peak phase of IOD events was observed in October/ November. The October and November SST anomalies of four strong dipole years 1961, 1994, 1996 and 1997 are shown in figure 5 and 6 respectively (where 1996 is a strong negative dipole year). The peak phases of eastern cooling during 1961 and 1994 were observed in October (figure 5) where as in November during 1997. In 1961 the model has simulated eastern cooling more than $2^oC$where as in HadISST cooling was observed up to 1.5^oC. November 1997 shows a basin wide warming of about 0.8^oC in the western tropical Indian Ocean and cooling of about 2^oC in south eastern tropical Indian Ocean. This is evident in both model and observations.

3.3 Subsurface Temperature variability

The maximum anomalies in temperature during IOD years are observed in the subsurface than in the surface. Figure 7 and 8 represents the comparison of model and SODA subsurface temperature anomalies [a. 1961, b. 1994 and c. 1997] for October and November along the equator. During November 1997 subsurface temperature anomalies exceeding 5^oC were seen both in model simulation and SODA. The maximum anomalies are observed around 80 - 100m depth. Western equatorial Indian Ocean shows maximum subsurface warming during 1994 November. Subsurface temperature anomalies above 2^oC were seen in the model and SODA data around 90m depth. During dipole mode events the intensity of cooling in the eastern Indian Ocean is stronger than the warming in the western Indian Ocean both in the surface and subsurface. In the peak phase of IOD, when eastern EIO shows subsurface variability of 4-5^oC, western EIO shows temperature anomaly less than 2^oC. The subsurface negative temperature anomalies in the eastern EIO were seen beyond depth of 150m and up to 70^oE during positive IOD events. Positive temperature anomalies exist west of 70^oE. The remarkable feature of subsurface temperature anomalies during IOD events is the existence of maximum anomalies in almost equal depth in both eastern and western basins.

3.4 Simulation of North and Equatorial Indian Ocean Circulation

The model simulated climatological surface currents for December/January, April/May, July/August and October/November are shown in figure 9 (Left Panel) and from SODA (in right panel). The semiannual occurrence of eastward Wyrtki Jets during transition periods April/ May and October/November are well simulated by the model. The Wyrtki Jets simulated by the model during spring season show magnitude of about 0.7 m/s between 70^oE and 80^oE and fall jets has magnitude of about 0.55 m/s between 60^oE to 70^oE. However the observations showed jet magnitudes of about 0.8 m/s during spring and 0.9 m/s during fall (Masson et al., 2002). The Wyrtki Jet observed in SODA climatology has magnitude of about 0.7m/s during spring and fall seasons. However the spatial pattern of the jets in the model simulation agrees very well with the observations. The climatological features like existence of strong Somali jet and south west monsoon

currents are evident in model simulations. The most spectacular feature of the Indian Ocean, the reversal of Somali Current during winter monsoon season, the southward flowing East Indian Coastal Current, the northward flowing West Indian Coastal Current and westward flowing winter monsoon currents are well described by the model simulation and are comparable with SODA data sets. The model' s ability to reproduce the climatological circulation in the Indian Ocean encouraged us to do more analysis in interannual time scales. As the ECCO currents are more reliable we chose them ahead of SODA currents for the available period (1992 – 2000). The model simulations are compared with ECCO simulations for 1994, 1996 and 1997 events. As the ECCO data sets are available only since 1992, SODA datasets are used for all the analysis prior to 1992. After the onset of IOD events remarkable transformation in the circulation pattern emerges around October.

Figure 10 and 11 represent the model simulated and ECCO surface currents for October 1996 to January 1997 and October 1997 to January 1998 respectively. Unlike Pacific and Atlantic Oceans during summer monsoon season north equatorial current reverses its direction and flows eastward and this constitutes the southwest monsoon current which persists up to September/October. By December the North Equatorial Current flows westward and eastward flowing equatorial counter current exists south of equator. However in positive IOD years north equatorial current weakens and confine to a narrow band and disappear in south of Sri Lanka. In contrast during 1996, the southwest monsoon current was more intense than normal. One remarkable feature observed during the positive dipole year is the absence or reversal of Wyrtki Jets. Strong westward currents exist in the region equator to 10^{o}S in 1961 October. In 1994, eastward flow seen in the region equator to 5^{o}N and up to 80^{o}E. During 1961 October/November the anomalous westward currents in the entire EIO has replaced the Wyrtki Jets. October 1994 eastward currents were observed north of equator up to 80^{o}E where as south of equator strong westward currents were seen east of 70^{o}E. However ECCO data showed westward currents up to 80^{o}E only. During 1961 and 1994, the Wyrtki Jets have been weakened near 75 - 80^{o}E, subsequently the western part of the jet took a cyclonic turn in the northern hemisphere.

During the positive IOD years the Indian Ocean upper layer circulation changes and shows some resemblance to Pacific and Atlantic Ocean circulation pattern. Pacific and Atlantic Oceans surface circulation is characterised by westward flowing north equatorial current in equatorial and northern region and eastward flowing equatorial under current. Figure 12 shows the vertical section of zonal currents along the equator for 1996 and 1997. The EIO is characterised by strong westward currents in the fall of 1997. These westward currents intruded up to 50 m depth. Below 50m depth strong eastward currents are observed. The maximum intensity of these currents is seen at 80^{o}E - 90^{o}E. In case of negative IOD year 1996, strong eastward currents are seen in the EIO. The circulation pattern of westward currents in the upper layer and eastward currents in the subsurface can establish a vertical - zonal circulation in EIO. Further analysis of the model vertical velocity shows strong positive anomaly in the eastern Indian Ocean and negative anomalies in the western region during positive IOD years (figure 13). This implies that positive dipole years are characterized by strong upwelling in eastern EIO and downwelling processes in the western EIO. The upwelling in the eastern EIO brings cold water from subsurface to the surface and there by negative temperature anomalies appears. Te weakening or reversal of Wyrtki Jets also aids this cooling by reducing the transport of warm water from central EIO to the south eastern EIO. However in negative IOD years eastern Indian Ocean shows negative anomaly and positive anomaly in the western part. But the intensity of these anomalies is comparatively less than positive phase of IOD.

4. Summary

The Indian Ocean Dipole mode denotes a major mode of basin scale variability in the tropical Indian Ocean. A well parameterised Ocean General Circulation model MOM4 is used to simulate the surface and subsurface features associated with IOD events. The model simulations are thoroughly validated with observational data and are comparable with SODA and ECCO data sets. The model seasonal SST and current climatologies are able to reproduce the climatological features in the Indian Ocean. The SST seasonal climatologies of model and Levitus show an rms difference of 0.39, 0.27, 0.39 and 0.32^{o}C for winter, spring, summer and fall season respectively. The model dipole mode index, which is defined as a measure of strength of IOD events, shows good agreement with HadISST index. The warming in the western tropical Indian Ocean and cooling in the south eastern tropical Indian Ocean were well captured by the model SST anomalies. During IOD events the maximum temperature anomalies were seen in the subsurface at around 80 -100m depth in the eastern and western basins. The IOD events are characterised by large variability in the circulation pattern of equatorial Indian Ocean. The positive dipole years are remarkably noted by the weakening or absence of Wyrtki Jets. During fall 1997 the Wyrtki Jets reverse its direction resulting strong westward currents. The model simulated currents show good agreement with ECCO currents.

The spatial pattern of temperature anomaly (temperature also) is well comparable with observational data. This strongly suggests that the model can be used for the detailed study of the dynamical and thermodynamical processes associated with the onset, growth and termination of IOD events.

Appendix A

The net surface heat flux is obtained using the equation

$Q = Q_{sw} - Q_{lw} - Q_{sh} - Q_{lh}$

Where Q_{sw} , Q_{lw} , Q_{sh} and Q_{lh} are net downward shortwave radiation, net downward longwave radiation, sensible heat flux and latent heat flux, respectively. The net shortwave radiation is calculated as

$$Q_{sw} = Q_I (1-\alpha),\ \alpha = surface\ albedo = 0.066$$
$$Q_I = downward\ \ shortwave\ radiation\ passes\ the\ bottom\ of\ the\ atmosphere$$

The net longwave radiation is given by

$$Q_{LW} = Q_A - \sigma (SST)^4$$
Q_A *is downward longwave radiation,*
σ *is Stefan – Boltzmann cons* $\tan t = 5.67 \times 10^{-8}\ W/m^2/K^4$
SST is mod *el SST*

The latent heat flux is

$$Q_{lh} = A_v \rho_a C_E \left(q(z_q) - q_{sat}(SST)\right)\left|\Delta \vec{U}\right|$$

The sensible heat flux is

$$Q_{sh} = \rho_a c_p C_H \left(\theta(z_\theta) - SST\right)\left|\Delta \vec{U}\right|$$

where ρ_a is near surface air density

C_E and C_H are transfer coefficients for evaporation and sensible heat

$\Delta\vec{U} = \vec{U}(z_u) - \vec{U_0}$ is the difference between wind at height z_u and the surface current

$\theta(z_\theta)$ and $q(z_q)$ are potential temperature and specific humidity at different heights (z_θ) and (z_q) respectively

c_p is the specific heat capacity of air

A_v is the latent heat of vaporisation.

Acknowledgements

The first author B. Thompson wishes to acknowledge CSIR, India for JRF/SRF fellowship. The financial support from Department of Ocean Development, Govt. of India is acknowledged. The authors acknowledge Dr. Stephan Griffies and Dr. P. S. Swathi for their support and discussions during model installation and integration. Acknowledgements are also due to GFDL for making MOM4 code available, NCAR, BADC, UMD, and ECCO for data sets. We acknowledge Dr. Gurfan Beig and Mrs. Suvarna Fadnavis for the permission to access the SGI Octane workstation during initial stages of model testing. The encouragement and support from Director, IITM is sincerely acknowledged. We acknowledge Dr. A. K. Sahai for his critical revision and comments which helped to improve this report.

REFERENCES

Annamalai, H., S.P. Xie, J.P. McCreary, and R. Murtugudde, 2003: Coupled Dynamics over Indian Ocean: spring initiation of the Zonal Mode, Deep Sea Res., Part II, 50, 2305 – 2330.

Behera, S.K., S. Krishnan, and T. Yamagata, 1999: Unusual ocean-atmosphere conditions in the tropical Indian Ocean during 1994, Geophys. Res. Lett., 26, 3001-3004.

Behera, S.K., P.S. Salvekar, and T. Yamagata, 2000: Simulation of Interannual SST variation in the tropical Indian Ocean, J. Clim., 13, 3487 – 3489.

Behera, S.K., and T. Yamagata, 2003: Impact of the Indian Ocean Dipole on the southern Oscillation, J. Meteorol. Soc. Jpn., 81, 169 – 177.

Bryan, K., and L.J. Lewis, 1979: A water mass model of the world ocean, J. Geophys. Res., 84, 2503 - 2517.

Bryan, K., 1969: A numerical method for the study of the circulation of the world ocean, J. Comput. Phys., 4, 347 – 376.

Godfrey, J.S., E.F. Bradle, P.A. Coppin, L. Pender, T.J. McDougall, E.W. Schulz, and I. Helmond, 1999: Measurements of upper ocean heat and freshwater budgets near a drifting buoy in the equatorial Indian Ocean, J. Geophys. Res., 104(C6), 13,269 - 13,302.

Griffies, S. M., M. J. Harrison, R. C. Pacnowski, and A. Rosati, 2003: A Technical Guide to MOM4. GFDL Ocean Group Technical Report No. 5, Princeton, NJ: NOAA/Geophysical Fluid Dynamics Laboratory.

Iizuka, S., T. Matsuura, and T. Yamagata, 2000: The Indian Ocean SST dipole simulated in a coupled general circulation model, Geophys. Res. Lett., 27, 3369 – 3372.

Large, W.G., J.C. McWilliams and S.C. Doney, 1994: Oceanic vertical mixing: A review and a model with a nonlocal boundary layer parameterization, Reviews of Geophysics, 32, 363 – 403.

Pacanowski, R.C., A. Gnanadesikan, 1998: Transient response in a z-level ocean model that resolves topography with partial-cells, Mon. Weather Rev, 126, 3248-3270.

Masson, S., P. Delecluse, J.P. Boulanger, and C. Menkes, 2002: A model study of the seasonal variability and formation mechanism of barrier layer in the eastern equatorial Indian Ocean, J. Geophys. Res., 107(c12), 8017, doi:10.1029/2001 JC000832.

Masson, S., C. Menkes, P. Delecluse, and J.P. Boulanger, 2004: Impacts of salinity on the eastern Indian Oceans during termination of the fall Wyrtki Jet, J. Geophys. Res., 108(c3), 3067, doi:10.1029/2001JC000833.

Murtugudde, R., and A.J. Busalacchi, 1999: Interannual variability of the dynamics and thermodynamics of the tropical Indian Ocean, J. Clim., 12, 2300-2326.

Murtugudde, R., J. McCreary, and A.J. Busalacchi, 2000: Oceanic processes associated with anomalous events in the Indian Ocean with relevance to 1997–1998. J. Geophys. Res., *105*, 3295–3306.

Nicholls, N., 1989: Sea Surface temperatures and Australian winter rainfall, J. Clim., 2, 965 - 973.

Rao, S.A., S.K. Behra, Y. Masumoto, and T. Yamagata, 2002: Interannual subsurface variability in the tropical Indian Ocean with a special emphasis on the Indian Ocean dipole, Deep Sea Res., Part II, 49, 1549 – 1572.

Rayner, N. A., D. E. Parker, E. B. Horton, C. K. Folland, L. V. Alexander, and D. P. Rowell, E. C. Kent, A. Kaplan, 2003:Global analyses of sea surface temperature, sea ice, and night marine air temperature since the late nineteenth century, J. Geophys. Res., 108, D14, 4407, doi:10.1029/2002JD002670.

Saji, N.H., B.N. Goswami, P.N. Vinayachandran, and T. Yamagata, 1999: A dipole mode in the tropical Indian Ocean, Nature, **401**, 360-363.

Saji, N.H., and T. Yamagata, 2003: Possible impacts of Indian Ocean dipole mode events on global climate, Clim. Res., 25, 151 - 169.

Vinayachandran, P.N., S. Iizuka, and T. Yamagata, 2002: Indian Ocean dipole mode events in an ocean General Circulation model, Deep Sea Res., Part II, 49, 1573 – 1596.

Waliser, D., R. Murtugudde, and L. Lucas, 2003: Indo-Pacific ocean response to atmospheric intraseasonal variability: 1. Austral summer and the Madden-Julian oscillation, J. Geophys. Res., C5, 3160, 10.1029/2002JC001620.

Webster P.J., A.M. Moore, J.P. Loschnigg, and R.R. Leben, 1999: Coupled ocean-atmosphere dynamics n the Indian ocean during 1997 – 1998, *Nature,* **401**,356-360.

Zubair, L., S. A. rao, and T. Yamagata, 2003: Modulation of Sri Lankan Maha rainfall by the Indian Ocean Dipole, Geophys. Res. Lett., 30(2), 1063, doi:10.1029/2002 GL015639.

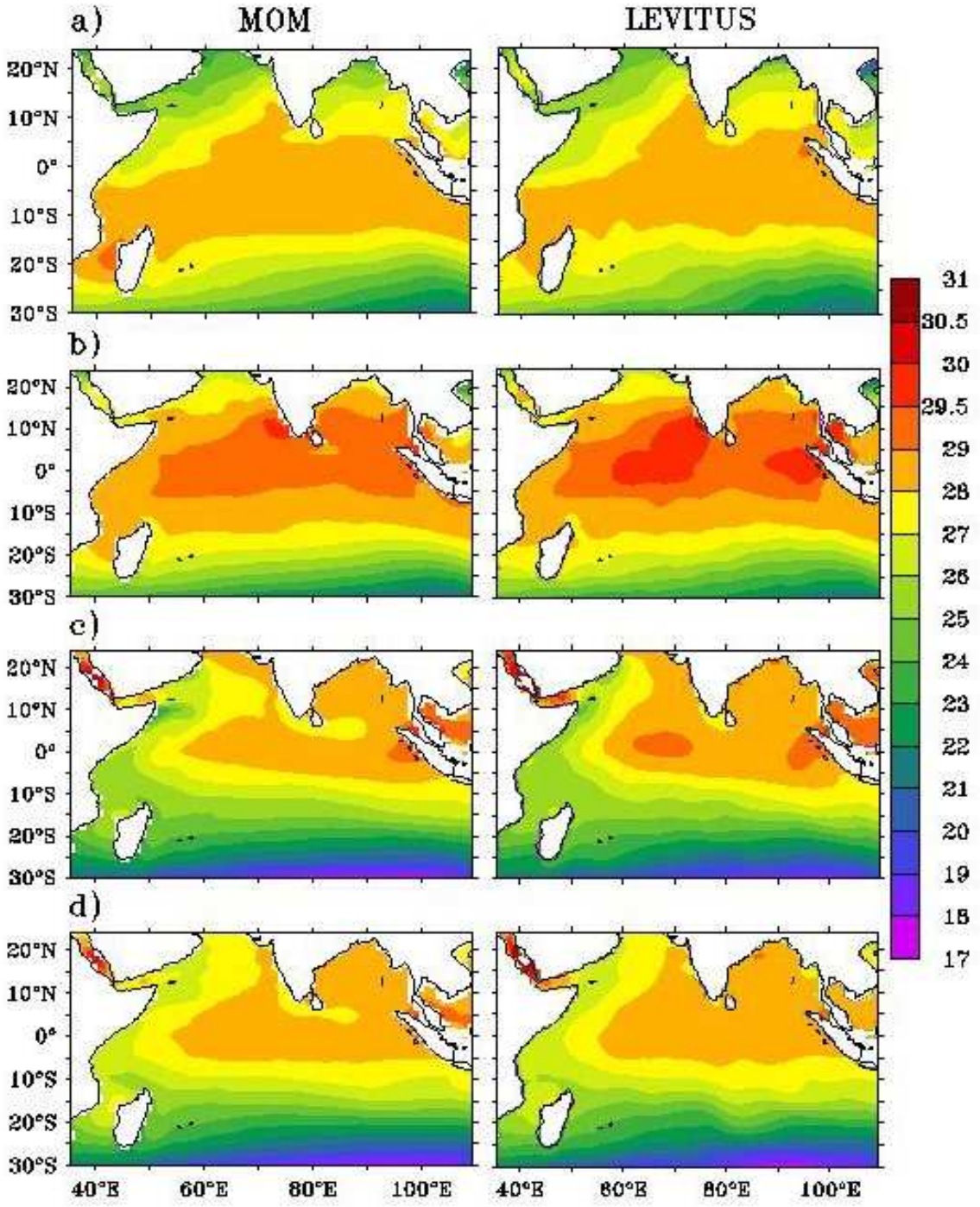

Figure 1. Seasonal SST climatology of model (1958-2000) and Levitus (1998) (a) Winter, (b) Spring, (c) summer, and (d) fall.

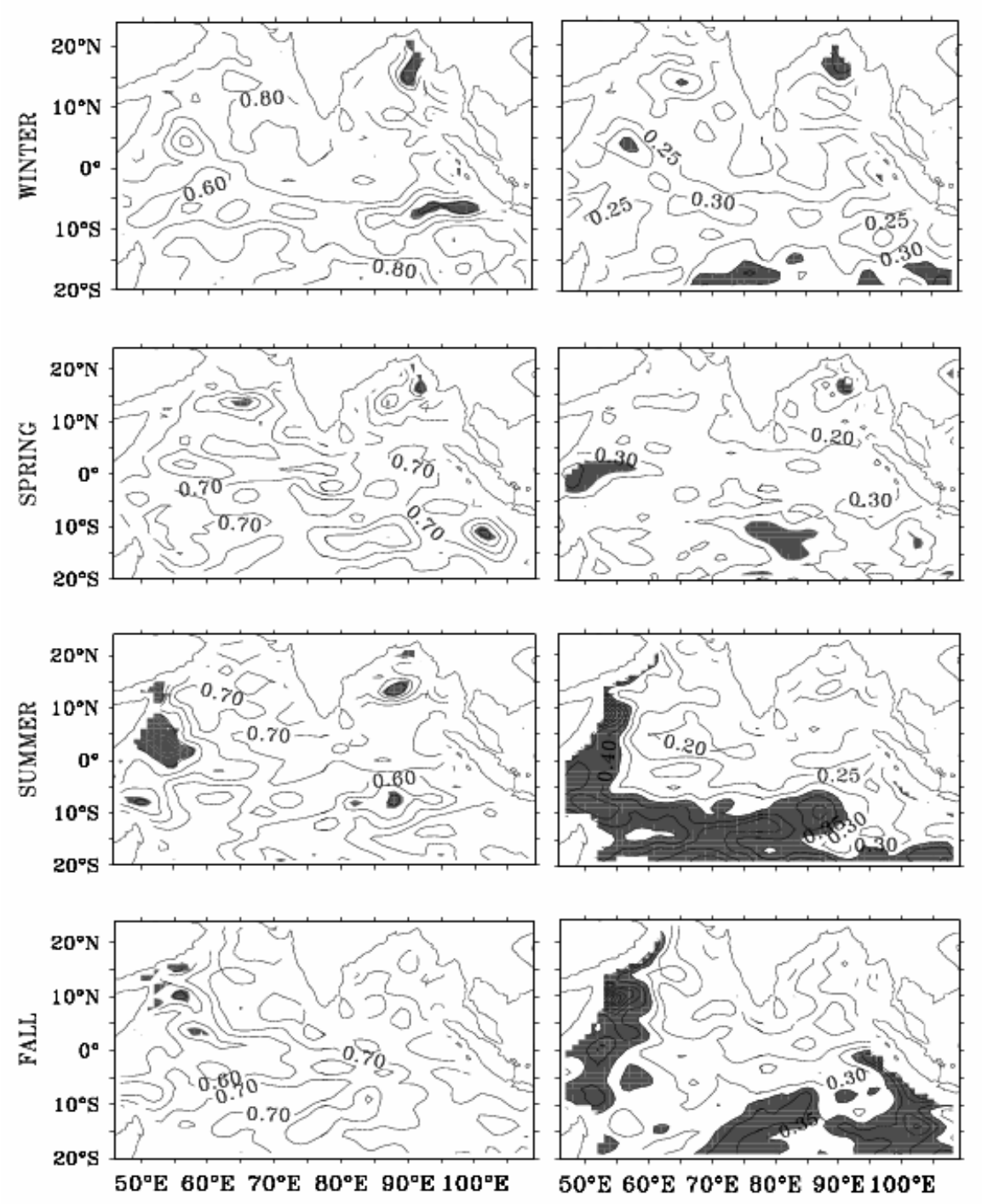

Figure 2. Left panel represents SST anomaly correlation between model and SODA (1958-2000) for winter, spring, summer and fall seasons. Correlation below 99% confidence level is shaded. Right panel shows the RMS difference between model and SODA. SST anomalies for the respective seasons (> 0.35^{o}C is shaded).

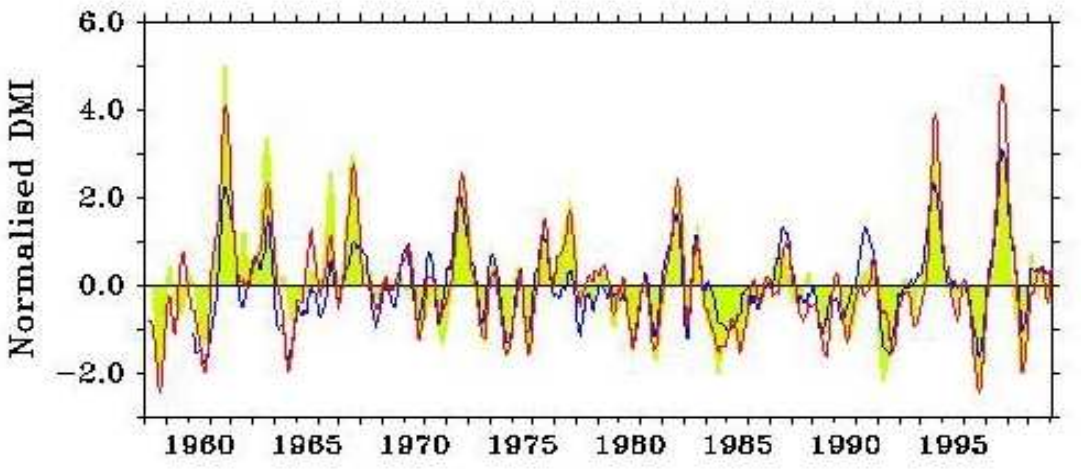

Figure 3. Normalised Dipole mode Index: Model (shaded) HadISST (blue line) and SODA (Red line).

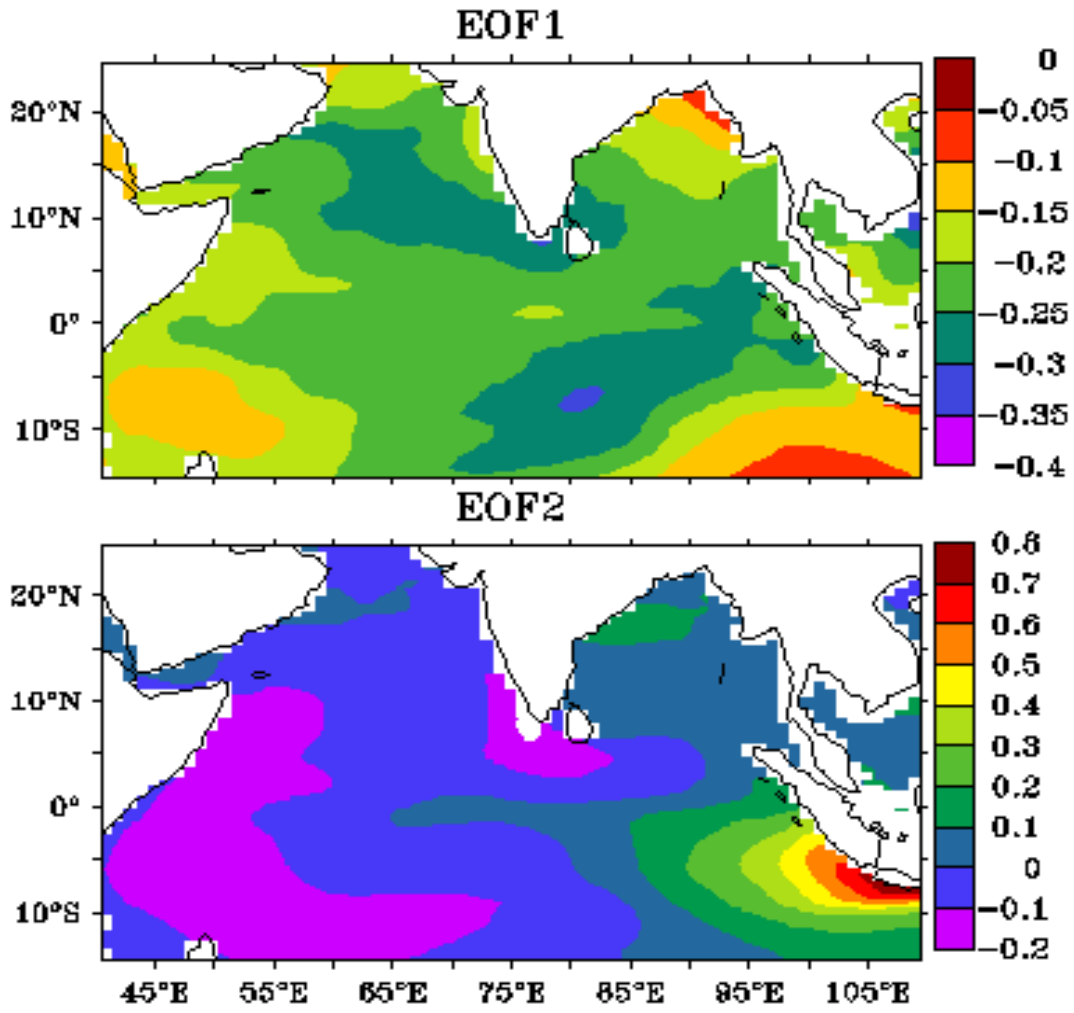

Figure 4. EOFs of model SST anomalies

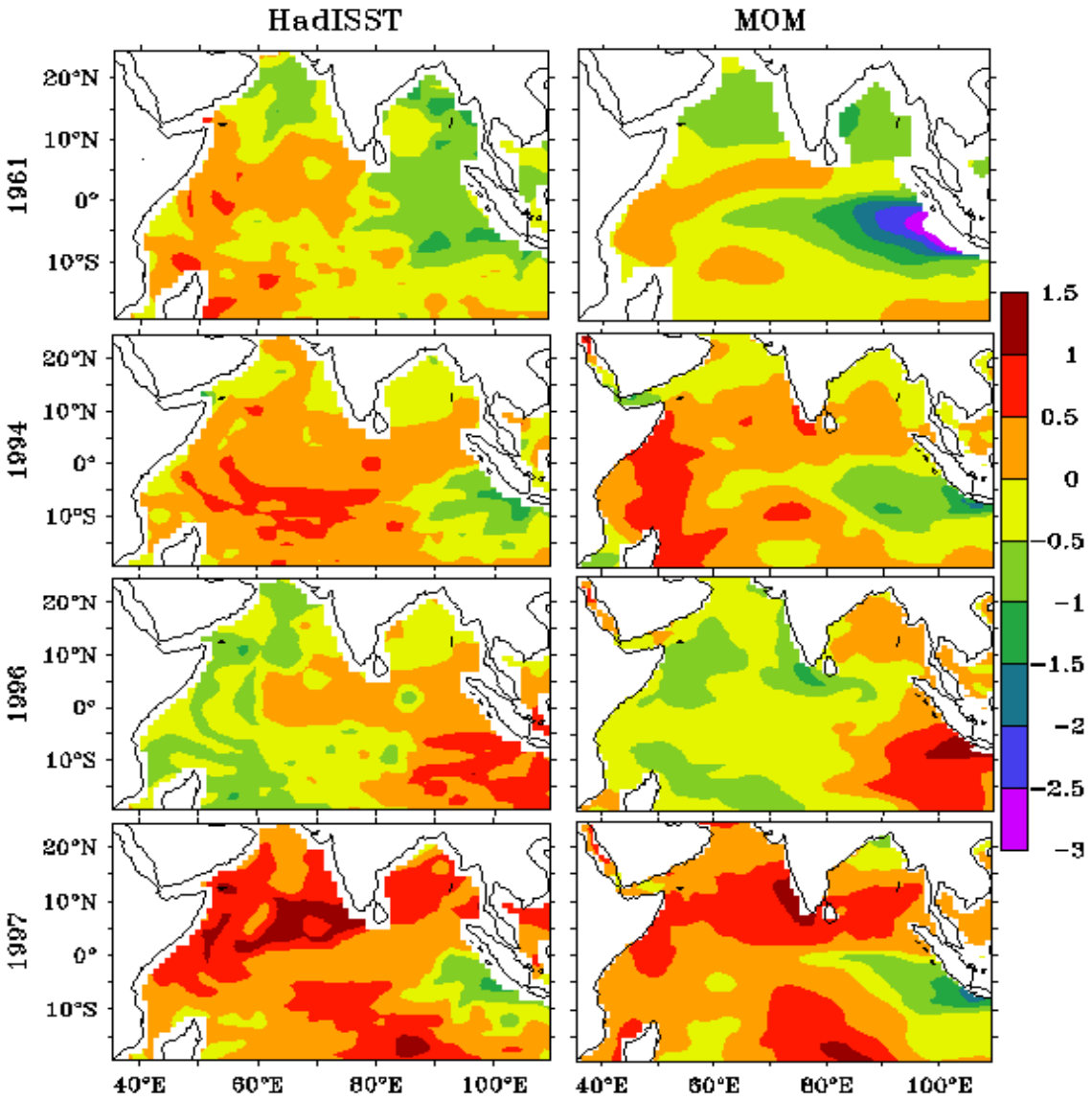

Figure 5. October SST anomalies for 1961, 1994, 1996 and 1997 HadISST and Model. Negative values are shaded

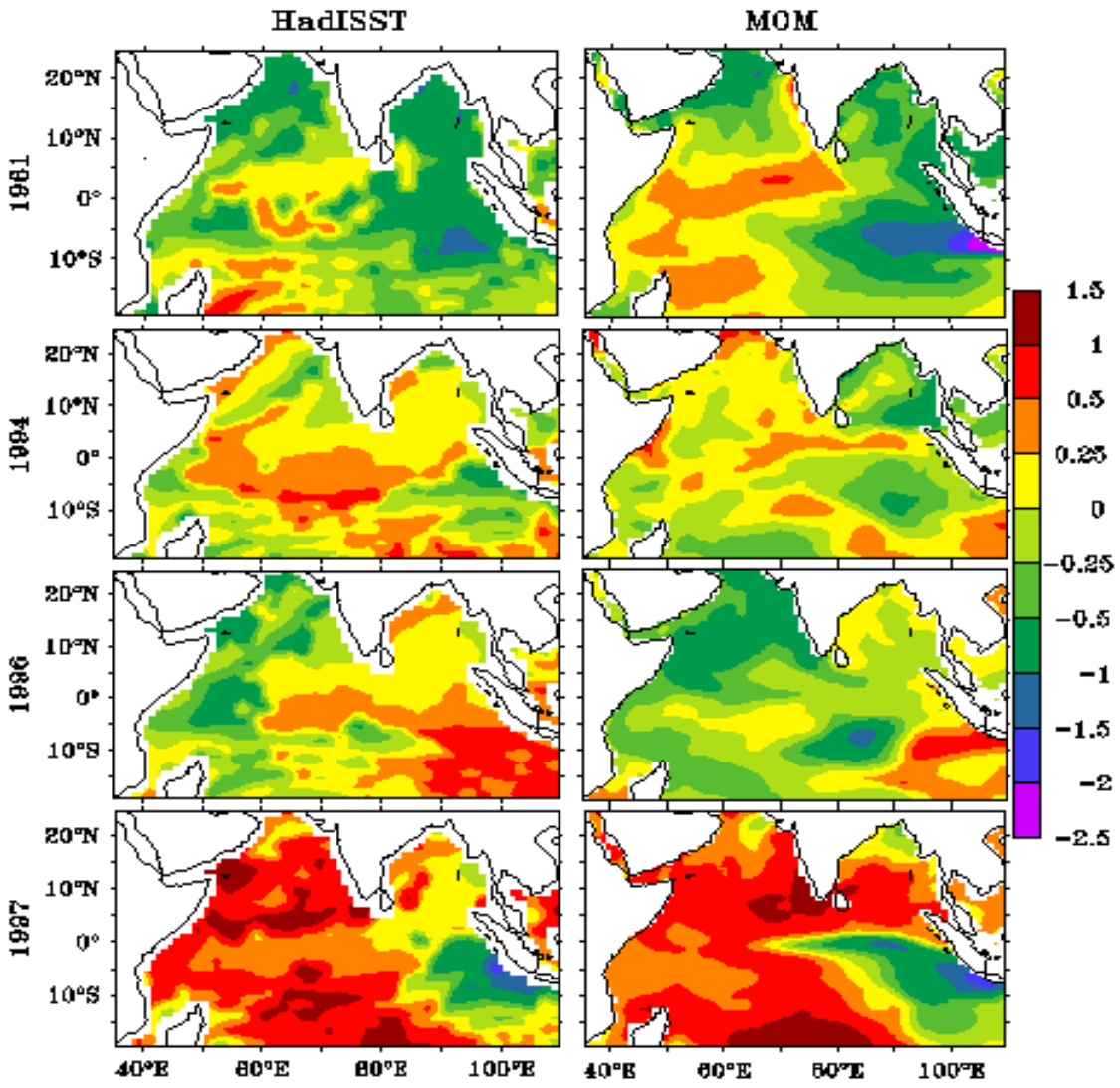

Figure 6. Same as figure 5. But for November.

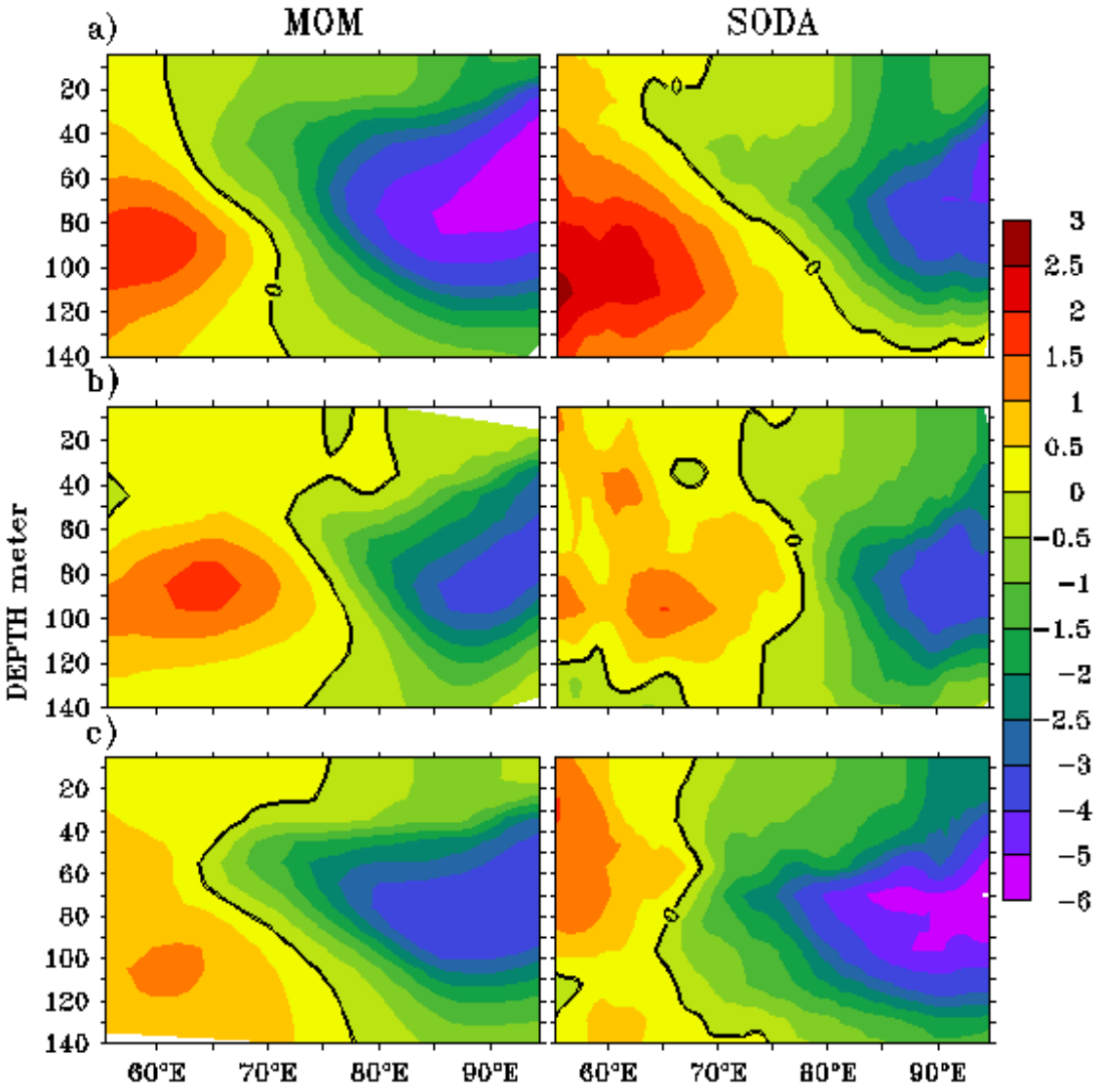

Figure 7. Subsurface temperature anomalies (October) along the equator from model and SODA. (a)1961, (b) 1994 and (c) 1997. Negative values are shaded.

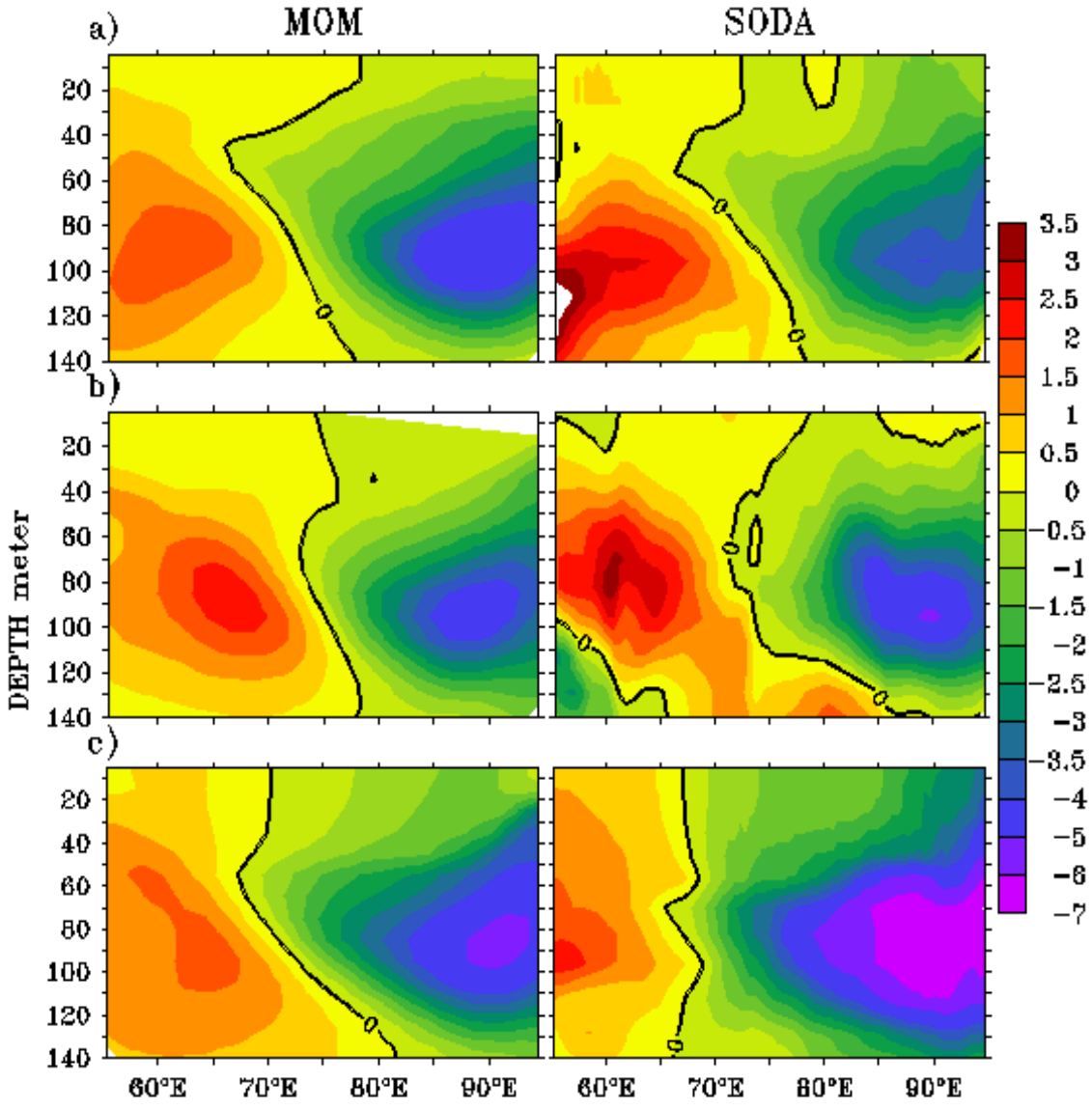

Figure 8. Same as figure 7, but for November.

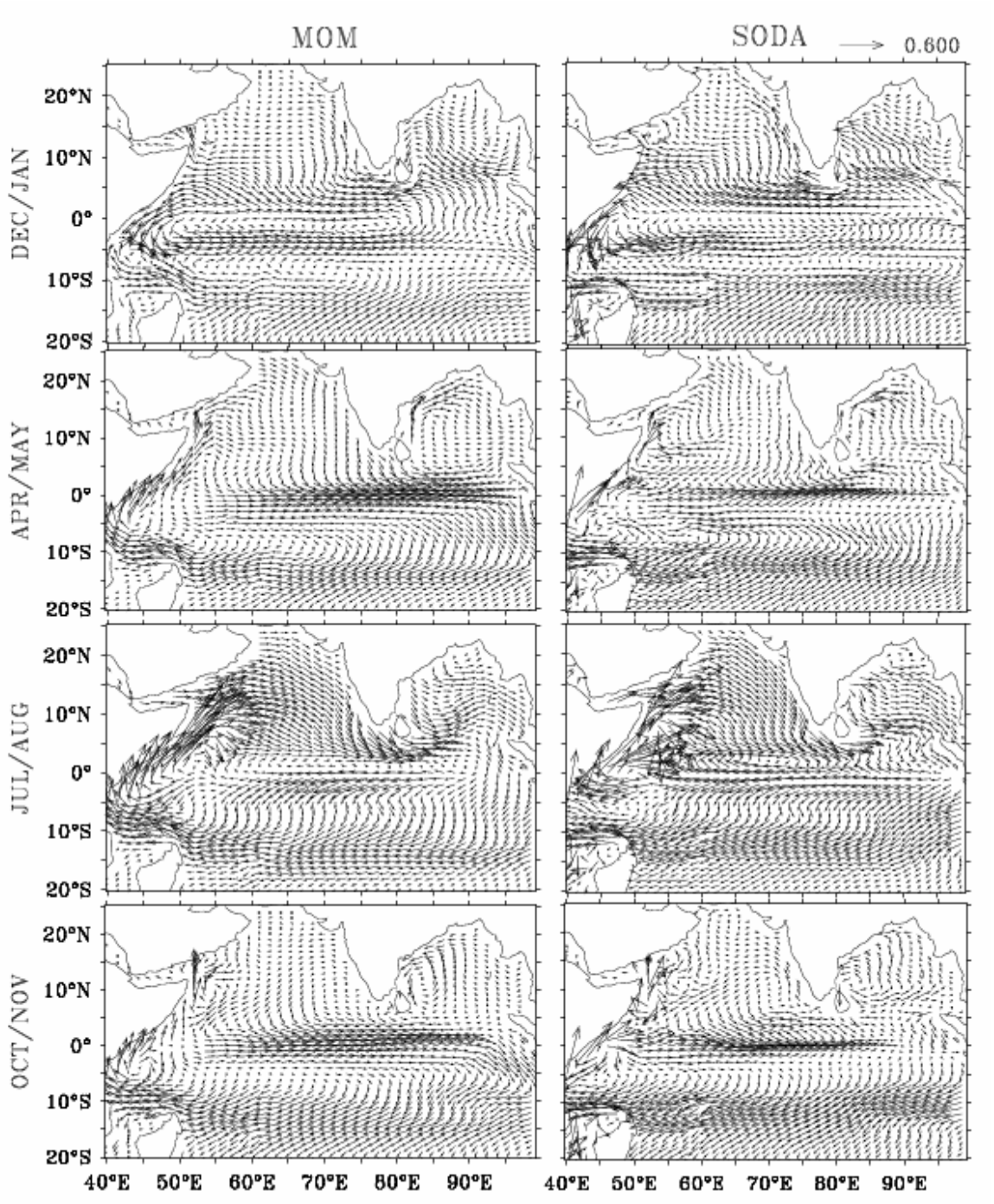

Figure 9. Surface current climatologies from model and SODA.

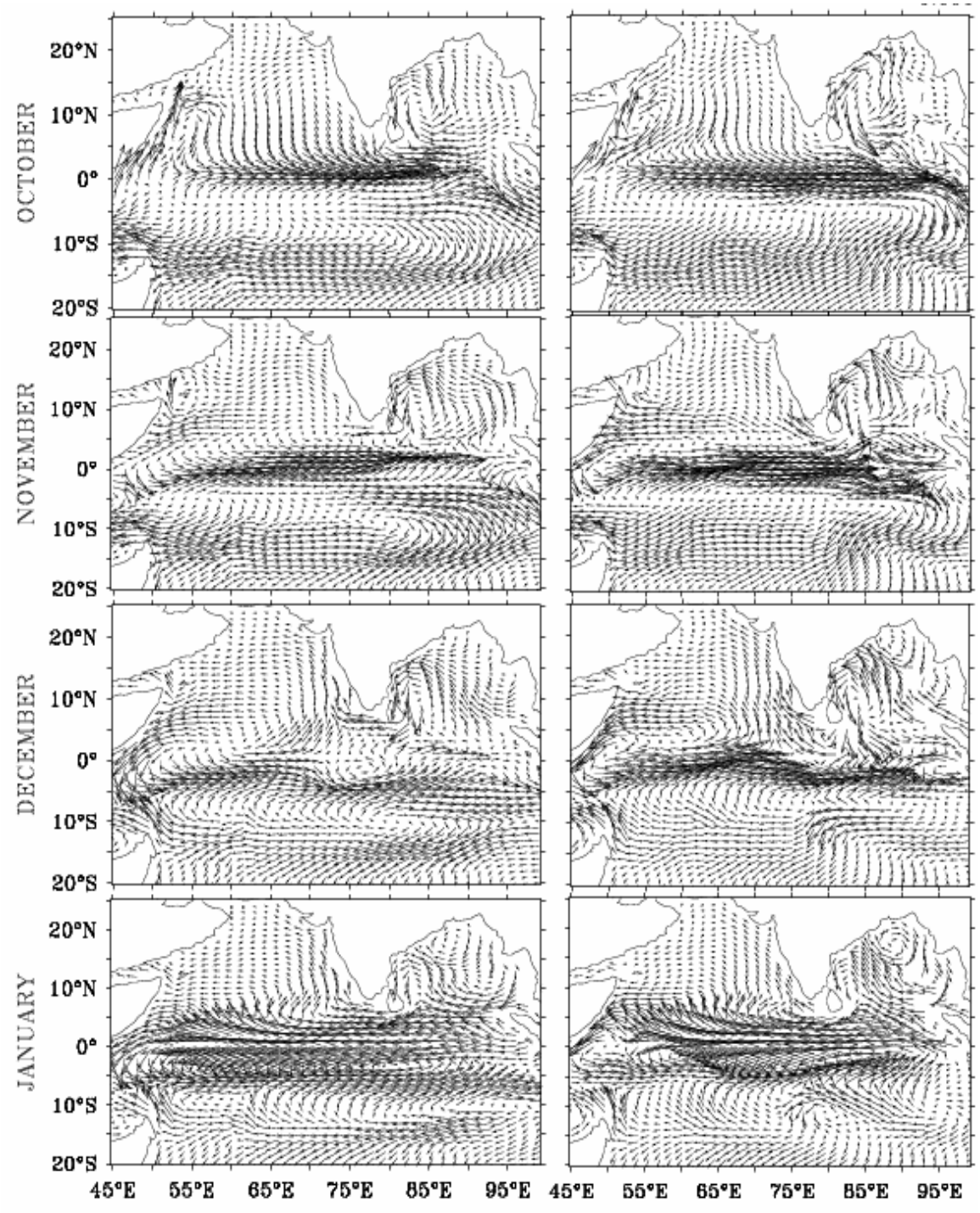

Figure 10. Surface currents from October 1996 to January 1997 model (Left) and ECCO (Right).

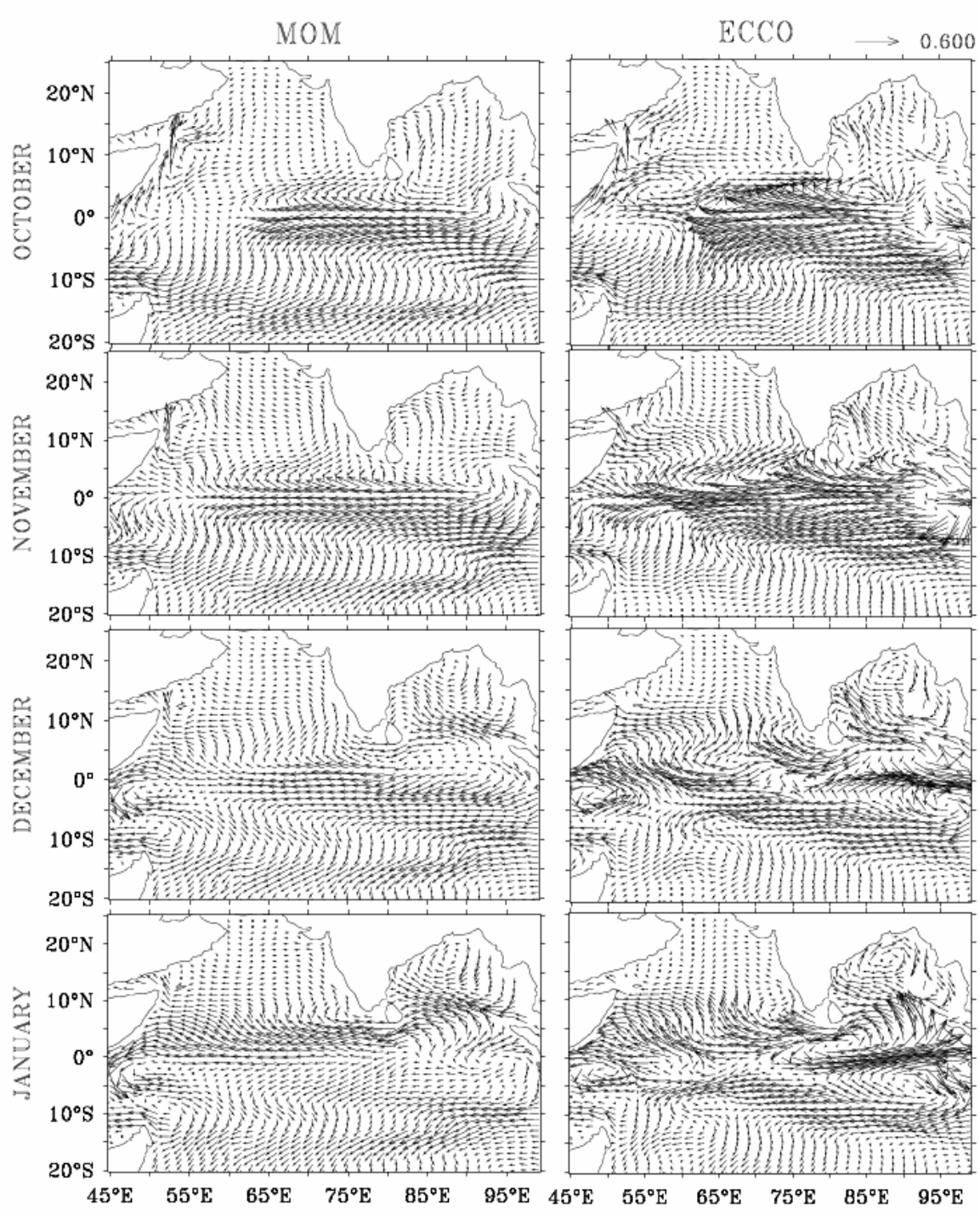

Figure 11. Surface currents from October 1997 to January 1998 model (Left) and ECCO (Right).

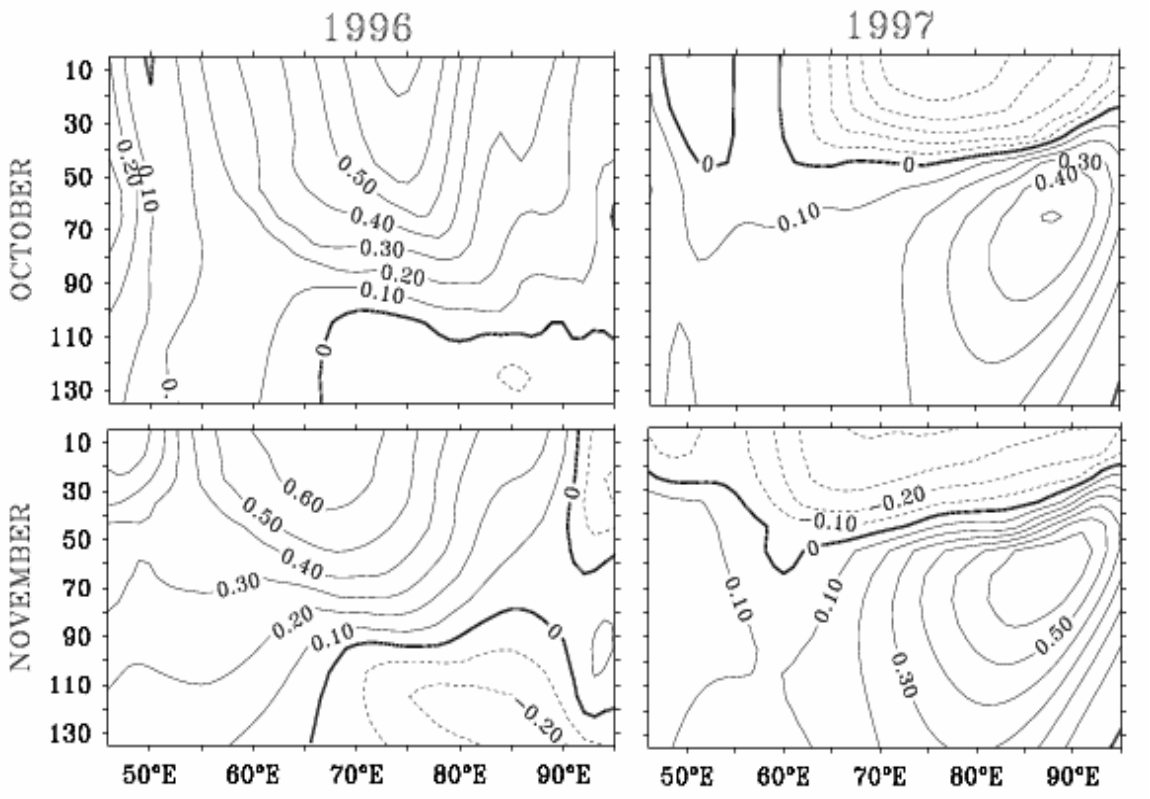

Figure 12. Vertical section of zonal currents along the equator for October and November. Left panel shows 1996 and right panel 1997.

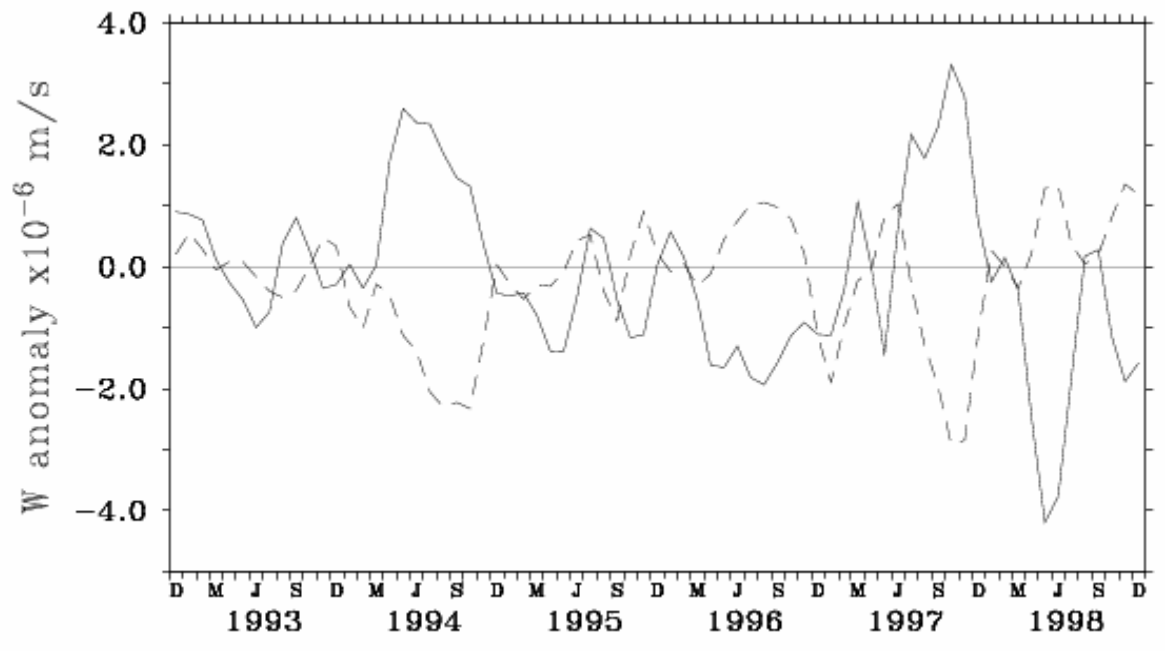

Figure 13. Vertical velocity anomalies at 50m from model. Thick line represents anomalies average in the eastern basin (90°E-110°E and 10°S–equator); dash represents anomalies averaged in the western basin (50°E-80°E and 10°S-equator).

I. I. T. M. RESEARCH REPORTS

- Energetic consistency of truncated models, Asnani G.C., August 1971, RR-001.
- Note on the turbulent fluxes of heat and moisture in the boundary layer over the Arabian Sea, Sinha S., August 1971, RR-002.
- Simulation of the spectral characteristics of the lower atmosphere by a simple electrical model and using it for prediction, Sinha S., September 1971, RR-003.
- Study of potential evapo-transpiration over Andhra Pradesh, Rakhecha P.R., September 1971, RR-004.
- Climatic cycles in India-1: Rainfall, Jagannathan P. and Parthasarathy B., November 1971, RR-005.
- Tibetan anticyclone and tropical easterly jet, Raghavan K., September 1972, RR-006.
- Theoretical study of mountain waves in Assam, De U.S., February 1973, RR-007.
- Local fallout of radioactive debris from nuclear explosion in a monsoon atmosphere, Saha K.R. and Sinha S., December 1972, RR-008.
- Mechanism for growth of tropical disturbances, Asnani G.C. and Keshavamurty R.N., April 1973, RR-009.
- Note on “Applicability of quasi-geostrophic barotropic model in the tropics”, Asnani G.C., February 1973, RR-010.
- On the behaviour of the 24-hour pressure tendency oscillations on the surface of the earth, Part-I: Frequency analysis, Part-II: Spectrum analysis for tropical stations, Misra B.M., December 1973, RR-011.
- On the behaviour of the 24 hour pressure tendency oscillations on the surface of the earth, Part-III : Spectrum analysis for the extra-tropical stations, Misra B.M., July 1976, RR-011A.
- Dynamical parameters derived from analytical functions representing Indian monsoon flow, Awade S.T. and Asnani G.C., November 1973, RR-012.
- Meridional circulation in summer monsoon of Southeast Asia, Asnani G.C., November 1973, RR-014.
- Energy conversions during weak monsoon, Keshavamurty R.N. and Awade S.T., August 1974, RR-015.
- Vertical motion in the Indian summer monsoon, Awade S.T. and Keshavamurty R.N., August 1974, RR-016.
- Semi-annual pressure oscillation from sea level to 100mb in the northernhemisphere, Asnani G.C. and Verma R.K., August 1974, RR-017.
- Suitable tables for application of gamma probability model to rainfall, Mooley D.A., November 1974, RR-018.

- Annual and semi-annual thickness oscillation in thenorthern hemisphere, Asnani G.C. and Verma R.K., January 1975, RR-020.

- Spherical harmonic analysis of the normal constant pressure charts in the northern hemisphere, Awade S.T., Asnani G.C. and Keshavamurty R.N., May 1978, RR-021.

- Dynamical parameters derived from analytical function representing normal July zonal flow along 87.5 °E, Awade S.T. and Asnani G.C., May 1978, RR-022.

- Study of trends and periodicities in the seasonal and annual rainfall of India, Parthasarathy B. and Dhar O.N., July 1975, RR-023.

- Southern hemisphere influence on Indian rainfall, Raghavan K.., Paul D.K. and Upasani P.U., February 1976, RR-024.

- Climatic fluctuations over Indian region - Rainfall : A review, Parthasarathy B. and Dhar O.N., May 1978, RR-025.

- Annual variation of meridional flux of sensible heat, Verma R.K. and Asnani G.C., December 1978, RR-026.

- Poisson distribution and years of bad monsoon over India, Mooley D.A and Parthasarathy B., April 1980, RR-027.

- On accelerating the FFT of Cooley and Tukey, Mishra S.K., February 1981, RR-028.

- Wind tunnel for simulation studies of the atmospheric boundary layer, Sivaramakrishnan S., February 1981, RR-029.

- Hundred years of Karnataka rainfall, Parthasarathy B. and Mooley D.A., March 1981, RR-030.

- Study of the anomalous thermal and wind patterns during early summer season of 1979 over the Afro-Asian region in relation to the large-scale performance of the monsoon over India, Verma R.K. and Sikka D.R., March 1981, RR-031.

- Some aspects of oceanic ITCZ and its disturbances during the onset and established phase of summer monsoon studied with Monex-79 data, Sikka D.R., Paul D.K. and Singh S.V., March 1981, RR- 032.

- Modification of Palmer drought index, Bhalme H.N. and Mooley D.A., March 1981, RR-033.

- Meteorological rocket payload for Menaka-II/Rohini 200 and its developmental details, Vernekar K.G. and Brij Mohan, April 1981, RR-034.

- Harmonic analysis of normal pentad rainfall of Indian stations, Anathakrishnan R. and Pathan J.M., October 1981, RR-035.

- Pentad rainfall charts and space-time variations of rainfall over India and the adjoining areas, Anathakrishnan R. and Pathan J.M., November 1981, RR-036.

- Dynamic effects of orography on the large scale motion of the atmosphere Part I : Zonal flow and elliptic barrier with maximum height of one km., Bavadekar S.N. and Khaladkar R.M., January 1983, RR-037.

- Limited area five level primitive equation model, Singh S.S., February 1983, RR-038.

- Developmental details of vortex and other aircraft thermometers, Vernekar K.G., Brij Mohan and Srivastava S., November 1983, RR-039.

- Note on the preliminary results of integration of a five level P.E. model with westerly wind and low orography, Bavadekar S.N., Khaladkar R.M., Bandyopadhyay A. and Seetaramayya P., November 1983, RR-040.
- Long-term variability of summer monsoon and climatic change, Verma R.K., Subramaniam K. and Dugam S.S., December 1984, RR-041.

- Project report on multidimensional initialization for NWP models, Sinha S., February 1989, RR-042.

- Numerical experiments with inclusion of orography in five level P.E. Model in pressure-coordinates for interhemispheric region, Bavadekar S.N. and Khaladkar R.M., March 1989, RR-043.

- Application of a quasi-lagrangian regional model for monsoon prediction, Singh S.S. and Bandyopadhyay A., July 1990, RR-044.

- High resolution UV-visible spectrometer for atmospheric studies, Bose S., Trimbake H.N., Londhe A.L. and Jadhav D.B., January 1991, RR-045.

- Fortran-77algorithm for cubic spline interpolation for regular and irregular grids, Tandon M.K., November 1991, RR-046.

- Fortran algorithm for 2-dimensional harmonic analysis, Tandon M.K., November 1991, RR- 047.

- 500 hPa ridge and Indian summer monsoon rainfall : A detailed diagnostic study, Krishna Kumar K., Rupa Kumar K. and Pant G.B., November 1991, RR-048.

- Documentation of the regional six level primitive equation model, Singh S.S. and Vaidya S.S., February 1992, RR-049.

- Utilisation of magnetic tapes on ND-560 computer system, Kripalani R.H. and Athale S.U., July 1992, RR-050.

- Spatial patterns of Indian summer monsoon rainfall for the period 1871-1990, Kripalani R.H., Kulkarni A.A., Panchawagh N.V. and Singh S.V., August 1992, RR-051.

- FORTRAN algorithm for divergent and rotational wind fields, Tandon M.K., November 1992, RR-052.

- Construction and analysis of all-India summer monsoon rainfall series for the longest instrumental period: 1813-1991, Sontakke N.A., Pant G.B. and Singh N., October 1992, RR-053.

- Some aspects of solar radiation, Tandon M.K., February 1993, RR-054.

- Design of a stepper motor driver circuit for use in the moving platform, Dharmaraj T. and Vernekar K.G., July 1993, RR-055.

- Experimental set-up to estimate the heat budget near the land surface interface, Vernekar K.G., Saxena S., Pillai J.S., Murthy B.S., Dharmaraj T. and Brij Mohan, July 1993, RR-056.

- Identification of self-organized criticality in atmospheric total ozone variability, Selvam A.M. and Radhamani M., July 1993, RR-057.

- Deterministic chaos and numerical weather prediction, Selvam A.M., February 1994, RR-058.

- Evaluation of a limited area model forecasts, Singh S.S., Vaidya S.S Bandyopadhyay A., Kulkarni A.A, Bawiskar S.M.,Sanjay J., Trivedi D.K. and Iyer U., October 1994, RR-059.

- Signatures of a universal spectrum for atmospheric interannual variability in COADS temperature time series, Selvam A.M., Joshi R.R. and Vijayakumar R., October 1994, RR-060.
- Identification of self-organized criticality in the interannual veriability of global surface temperature, Selvam A.M. and Radhamani M., October 1994, RR-061.

- Identification of a universal spectrum for nonlinear veriability of solar-geophysical parameters, Selvam A.M., Kulkarni M.K., Pethkar J.S. and Vijayakumar R., October 1994, RR-062.

- Universal spectrum for fluxes of energetic charged particles from the earth's magnetosphere, Selvam A.M. and Radhamani M., June 1995, RR-063.

- Estimation of nonlinear kinetic energy exchanges into individual triad interactions in the frequency domain by use of the cross-spectral technique, Chakraborty D.R., August 1995, RR-064.

- Monthly and seasonal rainfall series for all-India homogeneous regions and meteorological subdivisions: 1871-1994, Parthasarathy B., Munot A.A. and Kothawale D.R., August 1995, RR-065.

- Thermodynamics of the mixing processes in the atmospheric boundary layer over Pune during summer monsoon season, Morwal S.B. and Parasnis S.S., March 1996, RR-066.

- Instrumental period rainfall series of the Indian region: A documentation, Singh N. and Sontakke N.A., March 1996, RR-067.

- Some numerical experiments on roundoff-error growth in finite precision numerical computation, Fadnavis S., May 1996, RR-068.

- Fractal nature of MONTBLEX time series data, Selvam A.M. and Sapre V.V., May 1996, RR-069.

- Homogeneous regional summer monsoon rainfall over India: Interannual variability and teleconnections, Parthasarathy B., Rupa Kumar K. and Munot A.A., May 1996, RR-070.

- Universal spectrum for sunspot number variability, Selvam A.M. and Radhamani M., November 1996, RR-071.

- Development of simple reduced gravity ocean model for the study of upper north Indian Ocean, Behera S.K. and Salvekar P.S., November 1996, RR-072.

- Study of circadian rhythm and meteorological factors influencing acute myocardial infraction, Selvam A.M., Sen D. and Mody S.M.S., April 1997, RR-073.

- Signatures of universal spectrum for atmospheric gravity waves in southern oscillation index time series, Selvam A.M., Kulkarni M.K., Pethkar J.S. and Vijayakumar R., December 1997, RR-074.

- Some example of X-Y plots on Silicon Graphics, Selvam A.M., Fadnavis S. and Gharge S.P., May 1998, RR-075.

- Simulation of monsoon transient disturbances in a GCM, Ashok K., Soman M.K. and Satyan V., August 1998, RR-076.

- Universal spectrum for intraseasonal variability in TOGA temperature time series, Selvam A.M., Radhamani M., Fadnavis S. and Tinmaker M.I.R., August 1998, RR-077.

- One dimensional model of atmospheric boundary layer, Parasnis S.S., Kulkarni M.K., Arulraj S. and Vernekar K.G., February 1999, RR-078.

- Diagnostic model of the surface boundary layer - A new approach, Sinha S., February 1999, RR-079.

- Computation of thermal properties of surface soil from energy balance equation using force - restore method, Sinha S., February 1999, RR-080.
- Fractal nature of TOGA temperature time series, Selvam A.M. and Sapre V.V., February 1999, RR-081.

- Evolution of convective boundary layer over the Deccan Plateau during summer monsoon, Parasnis S.S., February 1999, RR-082.

- Self-organized criticality in daily incidence of acute myocardial infarction, Selvam A.M., Sen D., and Mody S.M.S., Feburary 1999, RR-083.

- Monsoon simulation of 1991 and 1994 by GCM : Sensitivity to SST distribution, Ashrit R.G., Mandke S.K. and Soman M.K., March 1999, RR-084.

- Numerical investigation on wind induced interannual variability of the north Indian Ocean SST, Behera S.K., Salvekar P.S. and Ganer D.W., April 1999, RR-085.

- On step mountain eta model, Mukhopadhyay P., Vaidya S.S., Sanjay J. and Singh S.S., October 1999, RR-086.

- Land surface processes experiment in the Sabarmati river basin: an overview and early results, Vernekar K.G., Sinha S., Sadani L.K., Sivaramakrishnan S., Parasnis S.S., Brij Mohan, Saxena S., Dharamraj T., Pillai, J.S., Murthy B.S., Debaje, S.B., Patil, M.N. and Singh A.B., November 1999, RR-087.

- Reduction of AGCM systematic error by Artificial Neural Network: A new approach for dynamical seasonal prediction of Indian summer monsoon rainfall, Sahai A.K. and Satyan V., December 2000, RR-088.

- Ensemble GCM simulations of the contrasting Indian summer monsoons of the 1987 and 1988, Mujumdar M. and Krishnan R., February 2001, RR-089.

- Aerosol measurements using lidar and radiometers at Pune during INDOEX field phases, Maheskumar R.S., Devara P.C.S., Raj P.E., Jaya Rao Y., Pandithurai G., Dani K.K., Saha S.K., Sonbawne S.M. and Tiwari Y.K., December 2001, RR-090.

- Modelling studies of the 2000 Indian summer monsoon and extended analysis, Krishnan R., Mujumdar M., Vaidya V., Ramesh K.V. and Satyan V., December 2001, RR-091.

- Intercomparison of Asian summer monsoon 1997 simulated by atmospheric general circulation models, Mandke S.K., Ramesh K.V. and Satyan V., December 2001, RR-092.

- Prospects of prediction of Indian summer monsoon rainfall using global SST anomalies, Sahai A.K, Grimm A.M., Satyan V. and Pant G.B., April 2002, RR-093.

- Estimation of nonlinear heat and momentum transfer in the frequency domain buy the use of frequency co-spectra and cross-bispectra, Chakraborty D.R. and Biswas M.K., August 2002, RR-094

- Real time simulations of surface circulations by a simple ocean model, Reddy P.R.C., Salvekar P.S., Ganer D.W. and Deo A.A., January 2003, RR-095

- Evidence of twin gyres in the Indian ocean : new insights using reduced gravity model by daily winds, Reddy P.R.C., Salvekar P.S., Ganer D.W. and Deo A.A., February 2003, RR-096

- Dynamical seasonal prediction experiments of the Indian summer monsoon, Mujumdar M., Krishnan R. and Satyan V., June 2003, RR-097

- Thermodynamics and dynamics of the upper ocean mixed layer in the central and eastern Arabian Sea, Gnanaseelan C., Mishra A.K., Thompson B. and. Salvekar P.S, August 2003, RR-098
- Measurement of profiles and surface energy fluxes on the west coast of India at Vasco-Da-Gama, Goa during ARMEX 2002-03, Sivaramakrishnan S., Murthy B.S., Dharamraj T., Sukumaran C. and Rajitha Madhu Priya T., August 2003, RR-099

- Time – mean oceanic response and interannual variability in a global ocean GCM simulation, Ramesh K.V. and Krishnan R., September 2003, RR-100

- Multimodel scheme for prediction of monthly rainfall over India, Kulkarni J.R., Kulkarni S.G., Badhe Y., Tambe S S., Kulkarni B.D. and Pant G.B., December 2003, RR-101

- Mixed layer and thermocline interactions associated with monsoonal forcing over the Arabian Sea, Krishnan R. and Ramesh K.V., January 2004, RR-102

- Interannual variability of Kelvin and Rossby waves in the Indian Ocean from TOPEX/ POSEIDON altimetry data, Gnanaseelan C., Vaid B.H., Polito P.S. and Salvekar P.S., March 2004, RR-103

- Initialization experiments over Indian region with a limited area model using recursive digital filters, Badyopadhyay S. and Mahapatra S., July 2004, RR-104

- Sensitivity of Indian monsoon rainfall to different convective parameters in the relaxed Arakawa-Schubert scheme, Pattanaik D.R. and Satyan V., October 2004, RR-105

- Simulation of tropical Indian ocean surface circulation using a free surface sigma coordinate model, Prem Singh and Salvekar P.S., December 2004, RR-106

- Dynamical ensemble seasonal forecast experiments of recent Indian summer monsoons : an assessment using new approach, Mandke S.K., Sahai A.K. and Shinde M.A., July 2005, RR-107